

## IMPACT OF PHASE SEPARATION ON WASTE GLASS DURABILITY

Carol M. Jantzen, John B. Pickett, Kevin G. Brown , and Thomas B. Edwards  
Westinghouse Savannah River Company  
Aiken, SC 29808

This document was prepared in conjunction with work accomplished under Contract No. DE-AC09-96SR18500 with the U. S. Department of Energy.

### DISCLAIMER

This report was prepared as an account of work sponsored by an agency of the United States Government. Neither the United States Government nor any agency thereof, nor any of their employees, makes any warranty, express or implied, or assumes any legal liability or responsibility for the accuracy, completeness, or usefulness of any information, apparatus, product or process disclosed, or represents that its use would not infringe privately owned rights. Reference herein to any specific commercial product, process or service by trade name, trademark, manufacturer, or otherwise does not necessarily constitute or imply its endorsement, recommendation, or favoring by the United States Government or any agency thereof. The views and opinions of authors expressed herein do not necessarily state or reflect those of the United States Government or any agency thereof.

This report has been reproduced directly from the best available copy.

Available to DOE and DOE Contractors from the Office of Scientific and Technical Information, P. O. Box 62 Oak Ridge, TN 37831; prices available from (423) 576-8401.

Available to the public from the National Technical Information Service, U.S. Department of Commerce, 5285 Port Royal Road, Springfield, VA 22161.

### ABSTRACT

Phase separation is shown to have an adverse and unpredictable effect on durability of borosilicate nuclear waste glasses. The glass chemistry and thermal history of the waste glass during solidification in a canister can impact the kinetics of phase separation and thus, the long term durability of a the glass. Although waste glasses contain 15-20 components, many of the components are present in minor amounts. Greater than >95% of the glass chemistry is dominated by the seven major components,  $\text{Na}_2\text{O}$ -  $\text{K}_2\text{O}$ - $\text{Li}_2\text{O}$ - $\text{SiO}_2$ - $\text{Al}_2\text{O}_3$ - $\text{B}_2\text{O}_3$ - $\text{Fe}_2\text{O}_3$ . Although the phase equilibria of this seven component system has never been studied, a compositionally dependent "Phase Separation Discriminator" was developed from a database of 88 High Level Waste (HLW) glasses shown experimentally to be homogeneous and 22 shown experimentally to be phase separated. This discriminator ensures that the HLW glasses produced in the Defense Waste Processing Facility (DWPF) are homogeneous and have predictable long term durability.

### INTRODUCTION

High-level liquid nuclear waste (HLLW) at the Savannah River Site (SRS) is being immobilized by vitrification into borosilicate glass. The glass is produced and poured into stainless steel canisters in the Defense Waste Processing Facility (DWPF) for ultimate geologic disposal. The canistered borosilicate waste glass must comply with the Waste Acceptance Product Specifications (WAPS) established by the U.S. Department of Energy. WAPS Specification 1.3 relates to the ability of the vitrification process to consistently control the final waste form durability, i.e., the stability of the glass against attack by water.

The durability of the final DWPF glass is predicted by analysis of vitrified melter feed prior to transfer of the feed to the melter. The composition analysis is used to calculate a predicted durability for the DWPF production glass from the durability model, THERMO™ where the acronym stands for Thermodynamic Hydration Energy Reaction Model [1]. In order to be fed to the melter, each batch of melter feed must produce a glass whose predicted durability response is more durable (by at least two standard deviations) than the benchmark waste glass identified in the DWPF Environmental Assessment (EA) based on ASTM C1285.

THERMO™ [1] is a first principles model that expresses the thermodynamic tendency of oxide species (components) in a glass to hydrate. THERMO™ only models the durability response of homogeneous glasses. Modeling of only homogeneous glasses avoids mixing different leaching mechanisms in one model. For example, homogeneous glasses undergo ion exchange and matrix dissolution while crystallized glasses undergo accelerated grain boundary dissolution and phase separated glasses undergo preferential soluble phase dissolution.. Crystallization and phase separation are normally detrimental to glass durability and are dependent on the volume fraction crystallized and/or the volume fraction phase separated. Since volume fraction is dependent on thermal history, and the thermal history of each canister is not identical, then mixed mechanism durability modeling of glass must be avoided.

Phase separated glasses are excluded in the THERMO™ process model based upon a compositionally derived phase separation discriminator. The basis for this additional product quality constraint, termed the homogeneity constraint, is described in this study.

## BACKGROUND

Liquid-liquid phase separation is the growth of two or more non-crystalline glassy phases each of which will have a different composition from the overall melt [2]. Phase separation in glasses generally takes the form of immiscible liquid phases which differ in chemical composition, density, and surface tension. If the liquid-liquid immiscibility is “quenched in” when the glass is cooled to room temperature, it is often termed “glass-in-glass” phase separation.<sup>1</sup>

---

<sup>1</sup> The two principle types of glass-in-glass phase separation are spinodal decomposition and homogeneous nucleation. Spinodal decomposition is small composition fluctuations (normally in the 20-500Å range) that cause the melt to separate into two phases spontaneously. The phase boundaries are diffuse and difficult to determine via electron microscopy. Homogeneous nucleation occurs when a critical size nucleus forms in the melt, it is not spontaneous in that a free energy barrier for the formation of the nucleus must be overcome. The phase boundaries are sharp and crystallization of the amorphous droplet phase often occurs [2].

Controlling the glass chemistry in compositional regions that avoid phase separation is key to controlling glass durability and processing. Factors such as the relative density of the two liquids, their viscosities, the interphase surface energy, and the melt conditions determine whether the two liquids separate on a gross macroscopic level resulting in two separate liquid layers in a melter or whether they may remain separated only on a microscopic scale [4].

Phase separation, if it occurs on a microscopic scale, has been shown to be detrimental to the stability and durability of nuclear waste glasses [1,5,6] because one of the immiscible phases is always more soluble than the other. Phase separation complicates modeling of glass durability as a function of composition, because the composition of the overall glass is known but the compositions of the two individual phases composing the glass is not known. If a glass is phase separated, the durability is dominated by the more soluble phase, causing the overall poorer durability of phase separated glasses (Figure 1).

Phase separation of the glass-in-glass type has been observed in multicomponent nuclear waste glasses (PNL77-107) containing >12 wt% B<sub>2</sub>O<sub>3</sub> [7], PNNL 76-68 containing 9.5 wt% B<sub>2</sub>O<sub>3</sub> [4], and a Hanford waste glass formulated by PNNL with 13.3 wt% B<sub>2</sub>O<sub>3</sub> [8]. Since waste glasses contain 15-20 components, phase separation in these complex systems is not well understood. However, many of the nuclear waste glass components are present in minor amounts and >95% of the glass chemistry is dominated by the seven major components, M<sub>2</sub>O-SiO<sub>2</sub>-Al<sub>2</sub>O<sub>3</sub>-B<sub>2</sub>O<sub>3</sub>-Fe<sub>2</sub>O<sub>3</sub>, where M = K + Na + Li.

Although the compositional dependency of phase separation in the individual M<sub>2</sub>O-SiO<sub>2</sub>-B<sub>2</sub>O<sub>3</sub> systems [9] and in the (M<sub>2</sub>O+MO)-(SiO<sub>2</sub>+Al<sub>2</sub>O<sub>3</sub>)-B<sub>2</sub>O<sub>3</sub> systems [9] where M<sub>2</sub>O is any alkali oxide and MO is any alkaline earth oxide are known, phase separation in the M<sub>2</sub>O-SiO<sub>2</sub>-Al<sub>2</sub>O<sub>3</sub>-B<sub>2</sub>O<sub>3</sub>-Fe<sub>2</sub>O<sub>3</sub> system has not previously been studied. Since both high level and low level waste

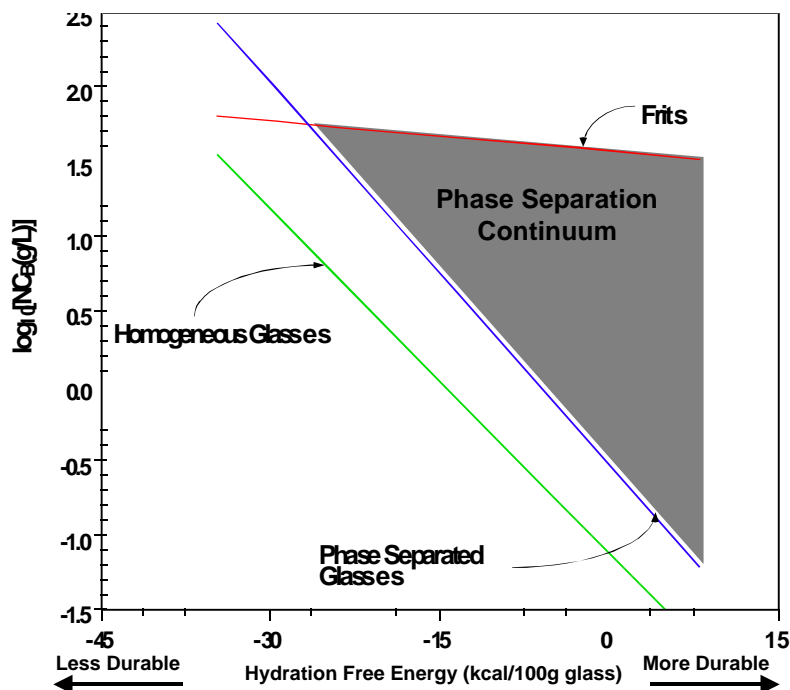


Figure 1. The first principles Thermodynamic Hydration Energy Reaction Model (THERMO™) distinguishes between the ASTM C1285 (PCT) response for phase separated glasses and homogeneous glasses. There appears to be a continuum of PCT response for phase separated glasses depending on the type and scale of the phase separation [1,10], e.g. phase separated waste glasses and phase separated frits give a different PCT response. In order to assure that the DWPF only processes homogeneous glasses, with predictable PCT responses, a phase separation discriminator or homogeneity constraint was developed and added to the Product Composition Control System (PCCS) [11] Statistical Process Control (SPC) system.

glasses contain  $\text{Fe}_2\text{O}_3$  as a significant component, phase separation in the seven component system  $\text{Na}_2\text{O}-\text{Li}_2\text{O}-\text{K}_2\text{O}-\text{SiO}_2-\text{Al}_2\text{O}_3-\text{B}_2\text{O}_3-\text{Fe}_2\text{O}_3$  is important to waste glass processing and glass durability.

## MODELING AND EXPERIMENTAL APPROACH

A well analyzed and well characterized set of 110 glasses was used to determine the boundary of the glass-in-glass immiscibility boundary in the seven component  $\text{Na}_2\text{O}-\text{Li}_2\text{O}-\text{K}_2\text{O}-\text{SiO}_2-\text{Al}_2\text{O}_3-\text{B}_2\text{O}_3-\text{Fe}_2\text{O}_3$  system. These homogeneous and phase separated glasses are designated as "Model Data" and are given by name and production mode in Table I. All glasses in "Model Data" met the following criteria: summed to  $100 \pm 5$  wt% oxide, were analyzed by Corning Engineering Laboratory Services (CELS) or bias corrected to CELS standards and contained 70-85wt% frit components.

An independent "Discriminator Validation Data" set was developed from glasses examined in this study and from the literature. The data was based on glass composition in oxide wt% and experimental observation of whether each glass was homogeneous or phase separated. Glasses in

the Discriminator Validation Data set often did not meet the stringent criteria that had been imposed on the “Model Data” set. The "Discriminator Validation Data" set does not contain any of the glasses from "Model Data" but does contain glasses that do not sum to  $100 \pm 5$  oxide wt%, contain greater than or less than 70-85 wt% frit components, and compositions that are as batched rather than as analyzed (as measured). The validation set of glasses is given in Table II. Table II indicates whether the individual glasses in the validation data set met the stringent criteria of “Model Data” or not. The “Validation Data Set” was used to validate the phase separation discriminator derived in this study.

The glasses in “Model Data” were fabricated under a variety of laboratory and pilot scale conditions by various researchers and vendors. Water quenching was used in the fabrication of many of the glass standards at Corning Engineering Laboratory Services (CELS). Water quenching is more rapid than air quenching, approximating quench rates of  $5 \times 10^4$  to  $1 \times 10^5$  °C/sec. Laboratory crucible melts were sometimes cooled by pouring the glass out of the crucible into a steel pan to represent the pouring of a small diameter melt stream in a pilot scale facility into a steel canister. Alternately, for small volume melts in ceramic and/or platinum crucibles the melts cooled rapidly enough in the crucibles that pouring was not necessary. All of these cooling histories are considered to be "air quenched" which yields a quench rate of  $10^{-1}$  to  $10^1$  °C/sec depending on the thermal conductivity and size of the sample.

The glasses in “Model Data” were either analyzed by (1) Corning Engineering Laboratory Services (CELS) or (2) by the Analytic Development Section (ADS) or the Engineering Test Facility (ETF) laboratory of SRTC using standards traceable to CELS. The number of replicate analyses performed varied from 2 to 10 depending on whether the glass was an unknown (duplicates) or a standard (10 replicates).

X-ray Diffraction (XRD) analysis was performed on all of the Model data set and Validation data set glasses studied. Scanning Electron Microscopy (SEM) analyses coupled with Energy Dispersive Analysis by X-ray (EDAX) were performed on glasses to identify crystalline species below the detection limit of XRD and to identify large scale phase separation. The EA glass was examined by optical microscopy, SEM, and TEM in order to determine the crystallinity and/or homogeneity of the glass on a microscopic level. Additional glasses such as Pyrex, the Batch 1 study glasses, the white frit 202 glass which had been remelted and cooled on a steel block, and the Hanford glasses were analyzed by Transmission Electron Microscopy (TEM) for phase separation.

## COMPOSITIONAL NATURE OF PHASE SEPARATION

In order to determine the compositional nature of the phase separation observed in the glasses in this study, it was necessary to examine the distribution of the oxide wt% concentrations of the homogeneous and phase separated glasses. Weight percent is used preferentially over normalized mole percents or mole fraction because glass-in-glass phase separation, including spinodal decomposition, is the separation of two immiscible phases that have different compositions and hence different densities [17-19]. Indeed, the dependence of the reciprocal of the density of each phase on the glass composition in weight percent is linear [17].

**Table I. Glasses Comprising “Model Data” Set**

<b>Glasses By Classification</b>	<b>No. of Glasses</b>	<b>Analytical Laboratory</b>
<b>Homogeneous Glasses</b>		
IDMS* Melter Hg Campaign	9	SRTC/ETF
AH Algorithm Glass Crucible Melts	29	CELS
DWPF Startup Frit, Fritted by Ferro	1	CELS
Waste Glass 202G and 202P Standards	2	CELS
Waste Glass 200R	1	SRTC/ADS
Waste Glass 165 CGW Standard	1	CELS
ARM-1 Approved Reference Glass	1	PNNL/MCC
Environmental Assessment Glass Standard	1	CELS
Waste Glass 131 TDS Crucible Melt	2	SRTC/ADS
Batch 1 Study 8,9,13,14,T Crucible Melt	5	SRTC/ADS
WCP Glass Standards		
Blend	1	CELS
Batch-1	1	CELS
Batch-2	1	CELS
Batch-3	1	CELS
Batch-4	1	CELS
HM	1	CELS
PX	1	CELS
IDMS* Melter Campaigns		
Blends-1	4	SRTC/ETF
Blends-2	5	SRTC/ETF
Blends-3	4	SRTC/ETF
IDMS* Melter Campaigns		
HM-1	4	SRTC/ETF
HM-2	3	SRTC/ETF
HM-3	3	SRTC/ETF
IDMS* Melter Campaigns		
PX-1	3	SRTC/ETF
PX-2	3	SRTC/ETF
<b>Phase Separated Glasses</b>		
IDMS* Melter Campaigns		
PX-4	3	SRTC/ETF
PX-5	9	SRTC/ETF
PX-6	1	SRTC/ETF
IDMS* Melter Campaigns PNNL Hanford (H) Glass	9	SRTC/ETF

<b>Totals</b>	<b>110</b>	<b>154</b>
---------------	------------	------------

**Table II. Composition-Based Discriminator Validation Data**

Sample ID	Type		Comment(s)
	Known	Predicted	
AH 168AL	$\phi$ Sep. <sup>t</sup>	$\phi$ Sep.	As Meas, Frit > 85%, SEM
PYREX	$\phi$ Sep.	$\phi$ Sep.	As Meas, Frit > 85%, Known f Sep.
NBS SRM 623	$\phi$ Sep.	$\phi$ Sep.	As Meas, Frit > 85%, TEM
MG-6	Homog.	Homog.	As Meas, TEM
MG-7	$\phi$ Sep.	$\phi$ Sep.	As Meas, Frit > 85%, TEM [12]
MG-9,18	Homog.	$\phi$ Sep.	As Meas, Frit > 85%, SEM [12]
MG-10,23,30	Homog.	Homog.	As Meas, Oxides(wt%) < 95%, SEM[12]
MG-17	Homog.	Homog.	As Meas, Oxides(wt%) > 105%, SEM [12]
MG-8,16,20,22,27 MG-29,32,33	Homog.	Homog.	As Meas, Frit < 70%, SEM [12]
Remaining 14 MG	Homog.	Homog.	As Meas, SEM [12]
FRIT 131,165	$\phi$ Sep.	$\phi$ Sep.	As Meas, Frit > 85%, SEM
FRIT 202	$\phi$ Sep.	$\phi$ Sep.	As Meas, Frit > 85%, SEM/TEM
CAC Glass 15,20	Homog.	Homog.	As Meas, TEM
CAC Glass 31	Homog.	Homog.	As Meas, Oxides(wt%) > 105%, TEM
Batch 1 Study 10,15	$\phi$ Sep.	$\phi$ Sep.	As Meas, Frit > 85%, TEM
PNL-77-268	$\phi$ Sep.	$\phi$ Sep.	As-Batched, Frit > 85%, TEM [7]
PNL-76-101	$\phi$ Sep.	$\phi$ Sep.	As-Batched, Frit > 85%, TEM [7]
PNL-77-269	$\phi$ Sep.	$\phi$ Sep.	As-Batched, TEM [7]
UK Glass M5 (189)	$\phi$ Sep.	$\phi$ Sep.	As-Batched, SANS [13]
PNL CVS-1-11	Homog.	Homog.	As-Batched/Meas., PNL SEM [5,14]
PNL CVS-2-30	Homog.	Homog.	As-Batched/Meas., PNL SEM [5,14]
PNL CVS-2-29	$\phi$ Sep.	$\phi$ Sep.	As-Batched/Meas., PNL SEM/TEM [5,14]
PNL CVS-2-31	$\phi$ Sep.	Homog.	As-Batched/Meas., PNL SEM/TEM [5,14]
Elmer Glass A,B	$\phi$ Sep.	$\phi$ Sep.	As-Batched, Frit > 85%, SEM [15]
Ventura Glass A,B	$\phi$ Sep.	$\phi$ Sep.	As-Batched, Frit > 85%, SEM [16]

<sup>t</sup> “ $\phi$  Sep.” indicates phase separated glasses.

Graphical histograms were used to compare the differences in the compositional distributions between the 88 homogeneous and 22 phase separated glasses given in Table I. The histogram analysis of the glass chemistry in oxide wt% indicated that the phase separated glasses were significantly lower in Al<sub>2</sub>O<sub>3</sub> while being somewhat higher in B<sub>2</sub>O<sub>3</sub> (Figure 2). The homogeneous glasses had about the same concentrations of Na<sub>2</sub>O, Li<sub>2</sub>O, SiO<sub>2</sub>, and K<sub>2</sub>O as the

phase separated glasses (Figure 1). Significant differences in the concentrations of other glass oxide components, e.g., CaO and FeO were not observed.

Visualization of the immiscibility region in the seven component  $\text{Na}_2\text{O}-\text{Li}_2\text{O}-\text{K}_2\text{O}-\text{SiO}_2-\text{Al}_2\text{O}_3-\text{B}_2\text{O}_3-\text{Fe}_2\text{O}_3$  system is difficult. In order to simplify the graphical representation  $\text{Na}_2\text{O}, \text{Li}_2\text{O}$ , and  $\text{K}_2\text{O}$  can be represented as one corner in the pseudoquaternary system.  $\text{M}_2\text{O}-(\text{SiO}_2+\text{Al}_2\text{O}_3)-\text{B}_2\text{O}_3-\text{Fe}_2\text{O}_3$  system. However, in this pseudoquaternary representation the high  $\text{SiO}_2$  and  $\text{Al}_2\text{O}_3$



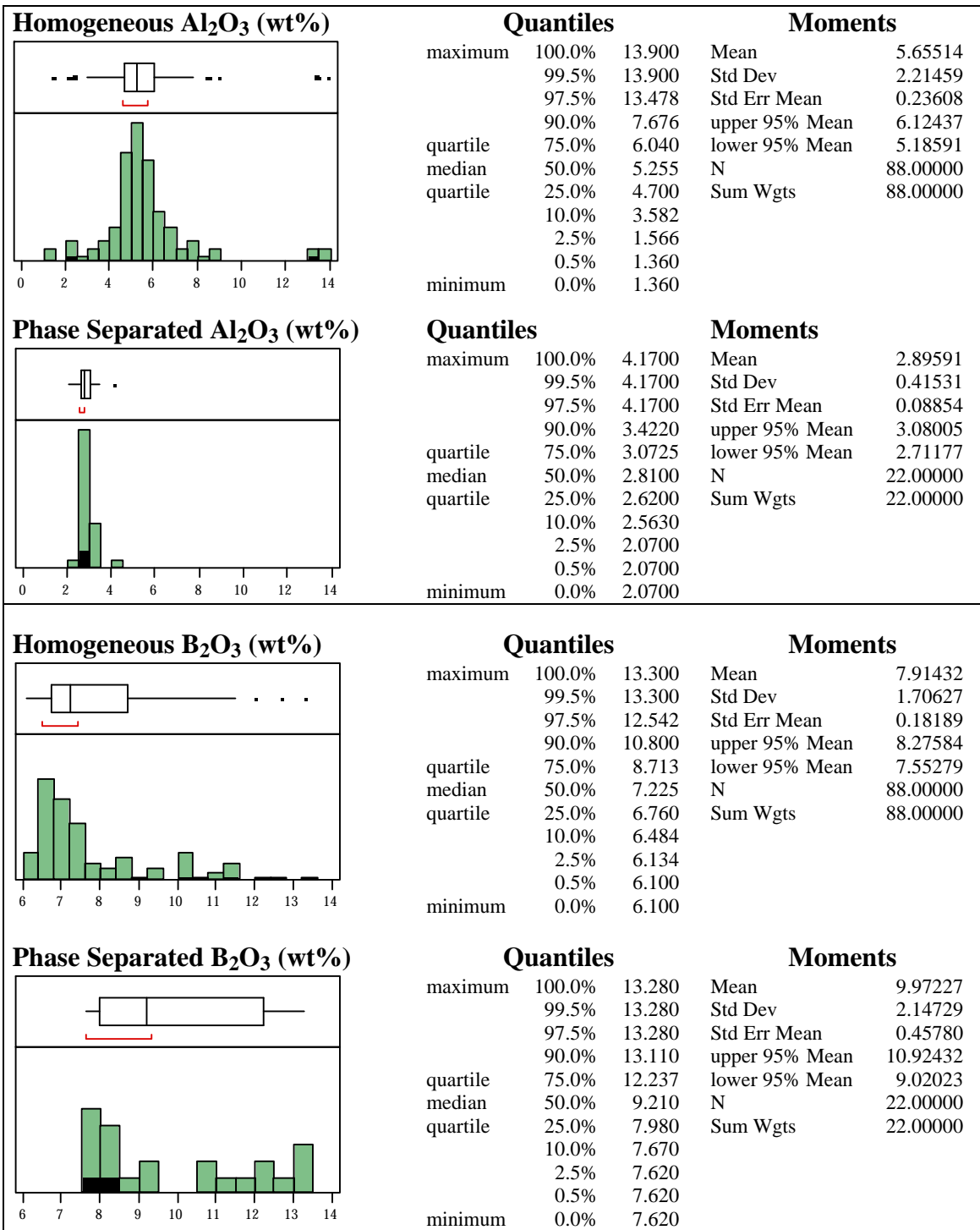


Figure 2. Histogram analysis of the compositional differences (in wt%) of phase separated and homogeneous glasses.

content of all these glasses cluster at the ( $\text{SiO}_2 + \text{Al}_2\text{O}_3$ ) apex. Alternatively, the  $\text{SiO}_2$  content of the 110 glasses was assumed to be approximately constant (varying only from 40 to 65 wt%) and the remaining elements renormalized and plotted in the pseudoquaternary system  $\Sigma\text{M}_2\text{O}$ - $\text{Fe}_2\text{O}_3$ - $\text{Al}_2\text{O}_3$ - $\text{B}_2\text{O}_3$  composition space (Figure 3). The shaded region in Figure 3 sharply delineates a compositional difference in weight percent composition space between the phase separated glasses and the homogeneous glasses: sharp phase boundaries in weight percent composition space are indicative of immiscibility boundaries.

Figure 2 indicates that the phase separated glasses are highly dependent on the  $\text{Al}_2\text{O}_3$  content of the glass. This is in agreement with the strong difference in the  $\text{Al}_2\text{O}_3$  concentration of the phase separated glasses and the homogeneous glasses noted in the oxide component distribution analysis (Figure 2). This is also in agreement with the widely known effects of increased  $\text{Al}_2\text{O}_3$  to stabilize glasses against phase separation [9]. It is also in agreement with the natural basalt analog quaternary system  $\text{Na}_2\text{O}$ - $\text{Al}_2\text{O}_3$ - $\text{Fe}_2\text{O}_3$ - $\text{SiO}_2$  shown in Figure 4 which depicts a region of immiscibility in alkali iron silicates with less than ~ 4 wt%  $\text{Al}_2\text{O}_3$  [20].

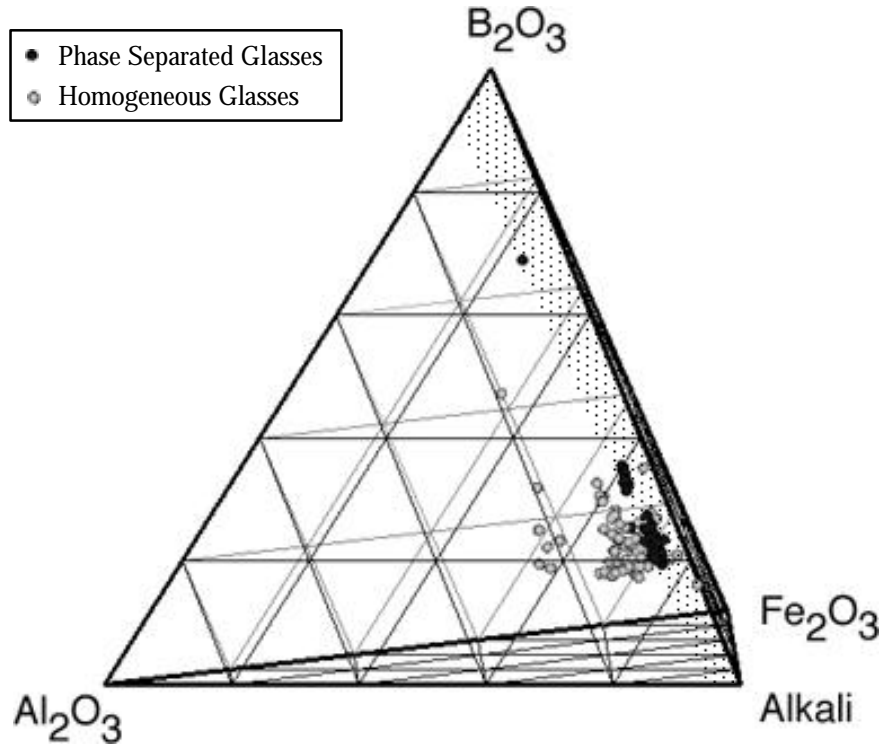


Figure 3. The homogeneous and phase separated glasses examined in this study plotted in  $\text{Al}_2\text{O}_3$ - $\text{B}_2\text{O}_3$ - $\Sigma\text{M}_2\text{O}$ - $\text{Fe}_2\text{O}_3$  composition space indicate that the phase separated glasses (shaded region) are low in  $\text{Al}_2\text{O}_3$  content relative to the homogeneous glasses.

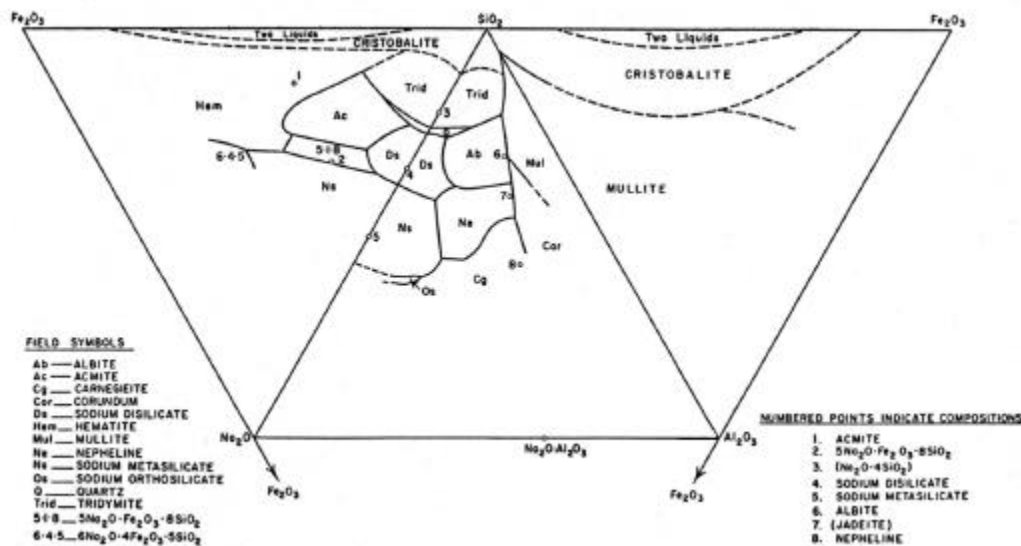


Figure 4. The quaternary system  $\text{Na}_2\text{O}-\text{Al}_2\text{O}_3-\text{Fe}_2\text{O}_3-\text{SiO}_2$  of geologic significance which shows the phase relations in this complex system. The three faces of the tetrahedron are shown laying flat in the plane of the base of the system (from reference 20) and there is a region of liquid-liquid immiscibility shown in the  $\text{Fe}_2\text{O}_3-\text{Al}_2\text{O}_3-\text{SiO}_2$  subsystem and the  $\text{Fe}_2\text{O}_3-\text{SiO}_2-\text{Na}_2\text{O}$  subsystem below  $\sim 4$  wt%  $\text{Al}_2\text{O}_3$ .

## DEVELOPMENT OF THE PHASE SEPARATION DISCRIMINATOR

Based on the oxide distribution analysis and the visualization of the homogeneous and inhomogeneous glass chemistry in the ternary  $\Sigma\text{M}_2\text{O}-(\text{SiO}_2+\text{Al}_2\text{O}_3)-\text{B}_2\text{O}_3$  [1] and quaternary  $\Sigma\text{M}_2\text{O}-\text{Al}_2\text{O}_3-\text{B}_2\text{O}_3-\text{Fe}_2\text{O}_3$  composition spaces (Figure 3) a compositional relationship for the phase separated vs. the homogeneous glasses was determined based primarily on the seven major components which dominate  $\geq 95\%$  of the glass chemistry, e.g.,  $\text{Na}_2\text{O}-\text{Li}_2\text{O}-\text{K}_2\text{O}-\text{Al}_2\text{O}_3-\text{B}_2\text{O}_3-\text{Fe}_2\text{O}_3-\text{SiO}_2$ .

Good discrimination between the homogeneous and phase separated glasses was achieved by plotting the sum of the lighter density alkali borosilicate (primarily frit ) components vs. the heavier density sludge components, e.g.  $\text{Al}_2\text{O}_3$  plus all of the iron present as  $\text{Fe}_2\text{O}_3$ . Calcium oxide,  $\text{MoO}_3$ , and the rare earths (i.e.,  $\text{Nd}_2\text{O}_3$ ,  $\text{Ce}_2\text{O}_3$ ,  $\text{La}_2\text{O}_3$ , and  $\text{Y}_2\text{O}_3$ ) were included as heavier density components to properly account for the sludge components.<sup>†</sup> Since the

<sup>†</sup> In this study, the  $\text{MoO}_3$  and rare earth oxides only occurred in the Hanford glasses including the ARM-1 reference glass although these species are also anticipated in DWPF glasses. Calcium oxide was included since it was present in most of the glasses,

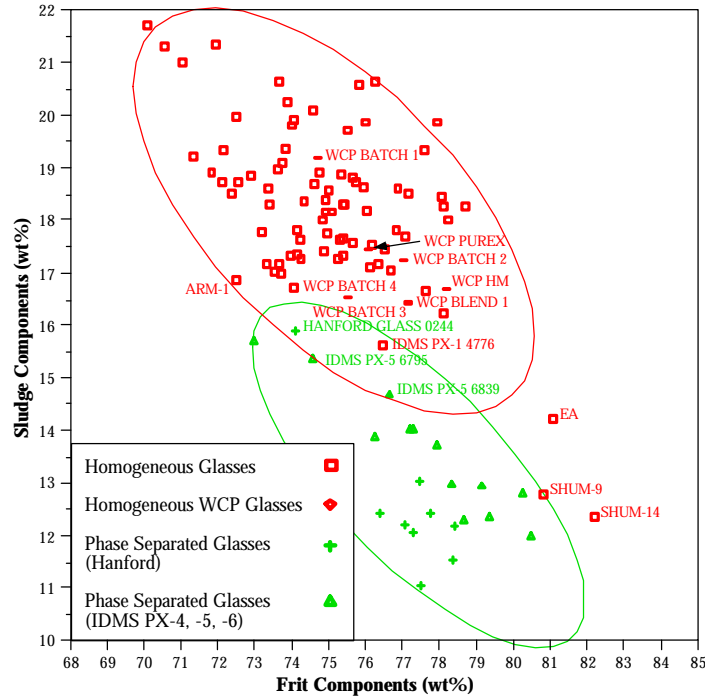
compositions of the glasses in this study were not statistically designed, certain minor sludge components (e.g., NiO, MnO, MgO, SrO, and ZrO<sub>2</sub>) were found to be insignificant to the discrimination and were thus omitted from the definition of the heavier density component.<sup>††</sup>

The discriminant analysis was generated in 14 dimensional (14 component) oxide wt% space. Figure 5 shows this representation in 2 dimensional space as overlapping ellipses. The discriminate function distinguishes between homogeneous and phase separated glasses on a compositional basis. Glasses will be homogeneous if the following criterion is satisfied:

$$-1.6035 x - 5.6478 y + 210.9203 < 0 \quad (1)$$

where  $y$  = Denser Components = Al<sub>2</sub>O<sub>3</sub> + (Fe<sub>2</sub>O<sub>3</sub> + FeO calculated as Fe<sub>2</sub>O<sub>3</sub>) + Nd<sub>2</sub>O<sub>3</sub> + Ce<sub>2</sub>O<sub>3</sub> + La<sub>2</sub>O<sub>3</sub> + Y<sub>2</sub>O<sub>3</sub> + CaO + MoO<sub>3</sub> (wt%)

$x$  = Less Dense Components = Na<sub>2</sub>O + Li<sub>2</sub>O + K<sub>2</sub>O + Cs<sub>2</sub>O + SiO<sub>2</sub> + B<sub>2</sub>O<sub>3</sub> (wt%)



including significant amounts in ARM-1, 200R, and the CGW 165 STD. Furthermore, CaO was included because it can play a role in phase separation in borosilicate glasses<sup>[9]</sup>.

<sup>††</sup> Many of these elements are highly correlated to the major sludge oxides, e.g., Al<sub>2</sub>O<sub>3</sub> and Fe<sub>2</sub>O<sub>3</sub>, and their inclusion tends to include considerable noise into the discrimination with minimal improvement.

Figure 5. Compositional distinction between homogeneous and phase separated glasses. 95% confidence ellipsoids are indicated for both the homogeneous and phase separated glasses.

Analysis of the distribution of the lighter components between the homogeneous and phase separated glasses in Table I indicates that the homogeneous glasses contain lower amounts of frit components than the phase separated glasses. The phase separated glasses are stabilized by a higher concentration of frit components ( $77.5 \pm 3.6$  wt%) than homogeneous glasses ( $75.2 \pm 4.4$  wt%).

## STATISTICAL VALIDATION OF THE PHASE SEPARATION DISCRIMINATOR

The results of the validation for the composition-based discriminant function represented by Equation 1 are summarized in Figure 6. Of the 53 validation glasses described in Table II, 34 were found homogeneous and 19 phase separated by either SEM, TEM, and/or SANS. Of the 34 known homogeneous glasses, 32 (or 94%) were correctly classified by Equation 1. Of the 19 known phase separated glasses, 18 (or 95%) were correctly classified. Note this is the more dangerous type of error as during production it is more conservative to err on the side of predicting a glass to be phase separated when it is not rather than vice versa. Thus approximately 95% of the glasses in Table II were discriminated appropriately despite the fact that only a few satisfied all the stringent “Model Data” criteria under which the discriminator was developed .

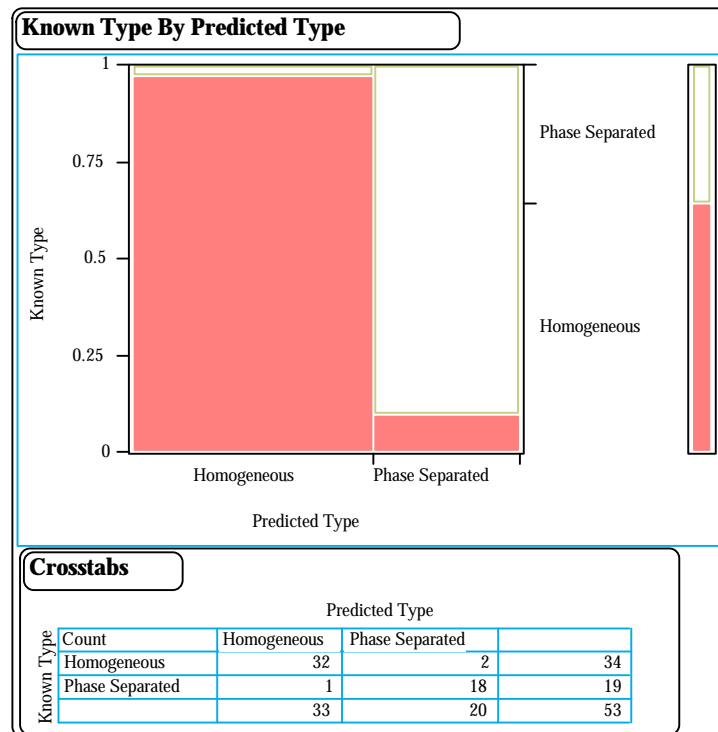


Figure 6. Results of the Phase Separation Composition Discriminator for DWPF and non-DWPF data.

## DISCUSSION

The need for a compositional phase separation discriminator to be used in conjunction with a glass durability model such as THERMO™ is apparent in the studies of Toven, et al [6] who demonstrated that the Jantzen/Plodinec free energy model [21] as well as the Feng/Barkatt enthalpy model [22-23] and the Bray/Yun [24-25] structural durability models did not predict waste glass durability accurately when the glasses contained >15% B<sub>2</sub>O<sub>3</sub> with little or no Al<sub>2</sub>O<sub>3</sub>. For these glasses all the previous models underpredicted the glass durability significantly. These authors [6] attributed the underprediction to phase separation and complete dissolution of the borate phase in the absence of alumina in the glass.

Glass durability cannot be predicted from composition unless the compositional regions of glass-in-glass phase separation are clearly delineated and avoided during waste glass processing. This was implemented by the DWPF prior to non-radioactive startup in 1994 by the addition of the phase separation discriminator (known as the homogeneity constraint) into the statistical process control system, PCCS, that is used to simultaneously produce durable and processable glass. This is illustrated graphically in Figure 7 where the durability, viscosity, liquidus and homogeneity constraints define the durable and processable DWPF waste glass compositions.

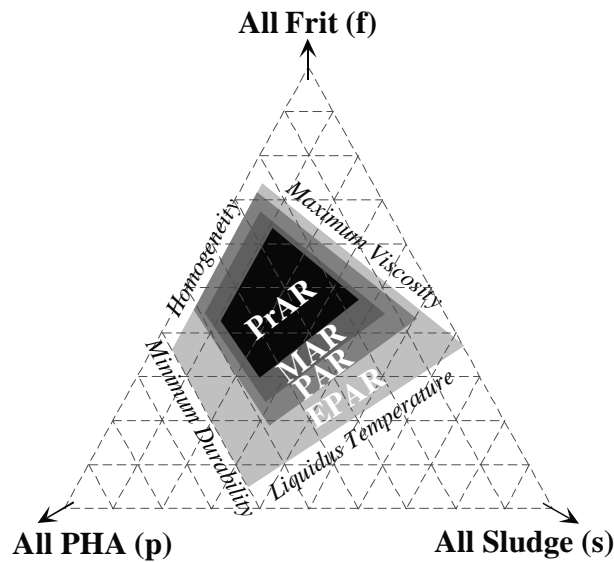


Figure 7. Schematic of the multiple constraints, including a glass homogeneity constraint, applied to the DWPF process to ensure with  $\geq 95\%$  confidence that homogeneous durable and processable glasses are produced.



## CONCLUSIONS

A region of liquid-liquid immiscibility is defined in a 14 component waste glass system in terms of a compositionally dependent phase separation discriminator. The discriminator function is defined in wt% and the two phases separating represent different melt densities. Glasses will be homogeneous if the following criterion is satisfied:

$$-1.6035 x - 5.6478 y + 210.9203 < 0 \quad (1)$$

where  $y$  = Denser Components =  $\text{Al}_2\text{O}_3 + (\text{Fe}_2\text{O}_3 + \text{FeO} \text{ calculated as } \text{Fe}_2\text{O}_3) + \text{Nd}_2\text{O}_3 + \text{Ce}_2\text{O}_3 + \text{La}_2\text{O}_3 + \text{Y}_2\text{O}_3 + \text{CaO} + \text{MoO}_3$  (wt%)

$x$  = Less Dense Components =  $\text{Na}_2\text{O} + \text{Li}_2\text{O} + \text{K}_2\text{O} + \text{Cs}_2\text{O} + \text{SiO}_2 + \text{B}_2\text{O}_3$  (wt%)

This constraint, when used to screen phase separated glasses out of a statistically designed study or out of a glass durability database, ensures that only homogeneous waste glass durability is being modeled. This also prevents mixed mechanism durability modeling which would otherwise allow phase separated waste glasses to be produced and durability to be incorrectly underpredicted.

## ACKNOWLEDGEMENT

This paper was prepared in connection with work done under Contract No. DE-AC09-96SR18500 with the U.S. Department of Energy.

## REFERENCES

1. C.M. Jantzen, J.B. Pickett, K.G. Brown, T.B. Edwards, U.S. Patent #5,846,278, "**Method of Determining Glass Durability (THERMO™)**" (December 8, 1998).
2. A Paul, "**Chemistry of Glasses**," Chapman & Hall, London, 293pp. (1982)
3. S.M. Ohlberg, H.R. Golob, and D.W. Strickler, "**Crystal Nucleation by Glass in Glass Separation**," in Symposium on Nucleation and Crystallization in Glasses and Melts, M.K. Reser, et.al. (Eds.), Am. Ceram. Soc., Columbus, OH, 55-62 (1962).
4. L.A. Chick, G.L. McVay, G.B. Mellinger, and F.P. Roberts, "**Annual Report on the Development and Characterization of Solidified Forms for Nuclear Wastes, 1979**" U.S. DOE Report PNL-3465, Battelle Pacific Northwest Laboratory (December, 1980).
5. P.R. Hrma, D.K. Peeler, et.al, "**Property/Composition Relationships for Hanford High-Level Waste Glass Melting at 1150°C**," U.S. DOE Report PNL-10359, Pacific Northwest Laboratory (December, 1994).
6. I. Toven, T. Advocat, D. GHaleb, E. Vernaz and F. Larche, "**Thermodynamic and Structural Models Compared with the Initial Dissolution Rates of SON Glass Samples**," Sci. Basis for Nucl. Waste Mgt., XVII, A. Barkatt and R.A. Van Konynenburg (Eds.), Materials Research Society, Pittsburgh, PA, 595-602 (1994).
7. M. Tomozawa, G.M. Singer, Y. Oka, and J.T. Warden, "Phase Separation in Nuclear Waste Glasses," *Ceramics in Nuclear Waste Management*, T.D. Chikalla and J.E. Mende. (Eds.), U.S. Dept. of Energy, Technical Information Center, Springfield, VA, CONF-790420, 193-196 (1979).

8. N.D. Hutson, "Integrated DWPF Melter System (IDMS) Campaign Report: Hanford Waste Vitrification Plan (HWVP) Process Demonstration," U.S. DOE Report, WSRC-TR-92-0403, Rev. 1, Westinghouse Savannah River Co., Aiken, SC (June, 1993).
9. M.B. Volf, "**Chemical Approach to Glass**," Glass Science and Technology, V. 7, Elsevier Science Publishing Co., Inc, New York, 594 pp (1984).
10. A.D. Cozzi and C.M. Jantzen, "Glass Durability Along the Compositional Continuum Between a Phase Separated Frit and a Homogeneous Glass," this p roceedings
11. R.L. Postles and K.G. Brown, "**The DWPF Product Composition Control System (PCCS) at Savannah River: Statistical Process Control Algorithm**," Ceramic Transactions, **23**, American Ceramic Society, Westerville, OH, 559-568 (1991).
12. W.G. Ramsey, "**Glass Dissolution Chemistry of the System  $\text{Na}_2\text{O-B}_2\text{O}_3\text{-SiO}_2\text{-Al}_2\text{O}_3\text{-Fe}_2\text{O}_3\text{-CaO}$** ," PhD Thesis, Clemson University, 202p (1995).
13. R.N. Sinclair, J.A. Erwin Desa, and A.D. Wright, "**Neutron Scattering Studies of Vitrified Radioactive Waste**," J. Am. Ceram. Soc., **66**[1], 72-77 (1983).
14. D.K. Peeler and P. Hrma, "**Compositional Range of Durable Borosilicate Simulated Waste Glasses**," Emerging Technologies in Hazardous Waste Management, V. VI, D.W. Tedder and F.G. Pohand, pp.323-338, American Academy of Environmental Engineers (1996).
15. T.H. Elmer, M.E. Nordberg, G.B. Carrier, and E.J. Korda, "**Phase Separation in Borosilicate Glasses as Seen by Electron Microscopy and Scanning Electron Microscopy**," J. Am. Ceram. Soc., **53**[4], 171-175 (1970).
16. P.C.S. Ventura, "**High Content Silicate Proous Glasses Used for Radioactive Wastes Storage: Preparation and Characterization of the Spinodal Decomposition**," Energy Research Abstracts, **19**[9], 282 (1995).
17. O.V. Mazurin and E.A. Porai-Koshits, "**Phase Separation in Glass**," North Holland Publishing Co., Amsterdam, 369p. (1984).
18. C.M. Jantzen, D. Schwahn, J. Schelten, and H. Herman, "**The  $\text{SiO}_2\text{-Al}_2\text{O}_3$  System, I. Later Stage of Spinodal Decomposition and Metastable Immiscibility**," Physics and Chemistry of Glasses, **22**[5], 122-137(1981).
19. C.M. Jantzen, D. Schwahn, J. Schelten, and H. Herman, "**The  $\text{SiO}_2\text{-Al}_2\text{O}_3$  System, II. The Glass Structure and Decomposition Model**," Physics and Chemistry of Glasses, **22**[5], 138-144 (1981).
20. D.K. Bailey and J.F. Schairer, "**The System  $\text{Na}_2\text{O-Al}_2\text{O}_3\text{-Fe}_2\text{O}_3\text{-SiO}_2$  at 1 Atmosphere, and the Petrogenesis of Alkaline Rocks**," Journal of Petrology, **7**[1], 114-170 (1966).
21. C.M. Jantzen, "**Thermodynamic Approach to Glass Corrosion**," Corrosion of Glass, Ceramics, and Ceramic Superconductors, D.E. Clark and B.K. Zaitos, Noyes Publications, Park Ridge, NJ, 153-215 (1992).
22. X. Feng, **Composition Effects on Chemical Durability and Viscosity of Nuclear Waste Glasses-Systematic Studies and Structural Thermodynamic Models**, Catholic University of America, PhD Thesis (1988).
23. X. Feng and A. Barkatt, "**Structural Thermodynamic Model for the Durability and Viscosity of Nuclear Waste Glasses**," Scientific Basis for Nuclear Waste Management, **XI**, M.J. Apted and R.E. Westerman (Eds.), Materials Research Society, Pittsburgh, PA, 543-554 (1987).
24. W.J. Dell and P.J. Bray, " **$^{11}\text{B}$  NMR Studies and Structural Modeling of  $\text{Na}_2\text{O-B}_2\text{O}_3\text{-SiO}_2$  Glass of High Soda Content**", J. Non-Crystalline Solids, **58**, 1-16 (1983).

25. Y.H. Yun and P.J. Bray, "**Nuclear Magnetic Resonance Studies of the Glasses in the System  $\text{Na}_2\text{O-B}_2\text{O}_3\text{-SiO}_2$** ," J. Non-Crystalline Solids, 27, 363-380 (1978).